Selective Bifunctional Modification of a Non-catenated Metal-Organic Framework Material via "Click" Chemistry

ARTICLE *in* JOURNAL OF THE AMERICAN CHEMICAL SOCIETY · OCTOBER 2009

Impact Factor: 12.11 · DOI: 10.1021/ja904189d · Source: PubMed

6 AUTHORS, INCLUDING:

Tendai Gadzikwa
University of Zimbabwe
10 PUBLICATIONS **675** CITATIONS
SEE PROFILE

Omar Farha
Northwnorthern University
211 PUBLICATIONS **12,159** CITATIONS
SEE PROFILE

Joseph Hupp
Northwestern University
521 PUBLICATIONS **29,507** CITATIONS
SEE PROFILE

Sonbinh Nguyen
Northwestern University
291 PUBLICATIONS **34,167** CITATIONS
SEE PROFILE

J|A|C|S COMMUNICATIONS

Published on Web 09/09/2009

Selective Bifunctional Modification of a Non-catenated Metal−Organic Framework Material via "Click" Chemistry

Tendai Gadzikwa, Omar K. Farha, Christos D. Malliakas, Mercouri G. Kanatzidis, Joseph T. Hupp,* and SonBinh T. Nguyen*

Department of Chemistry and the Institute for Catalysis in Energy Processes, Northwestern University, 2145 Sheridan Road, Evanston, Illinois 60208-3113

Received May 23, 2009; E-mail: j-hupp@northwestern.edu; stn@northwestern.edu

While the naming of the field of metal−organic frameworks (MOFs) alludes to the pivotal role played by organic chemistry in its study, there is a noticeable want of participation by organic chemists in the area of MOF-based materials. This has translated to a comparative neglect of two of the most powerful attributes of MOFs: their chemical versatility and their tailorability. Barring a few exceptions,[1] major MOF applications such as gas storage and separation have employed organic struts primarily as structural elements, holding the metal nodes apart to create pores of specific dimensions.[2] Although the incorporation of chiral ligands and the heterogenization of catalysts into MOFs are major steps toward giving the organic components more functional roles,[3] the true potential of the organic constituents had not been widely appreciated until recent developments in the area of post-synthesis modification (PSM) of MOFs.[4−6] Organic linkers have been chemically reduced to enhance the interactions of MOFs with H_2,[7] modified to integrate transition metal-based catalysts into MOFs[8] and to alter MOFs' macroscopic properties,[9] and elaborated to incorporate moieties that are inaccessible through traditional synthesis.[4] However, while MOFs can be synthetically modified in the same ways as small molecules, they are still microporous solids, with all the inherent properties of such materials. In this report, we take advantage of both the molecular and "macromolecular" aspects of MOFs to functionalize the interior and exterior surfaces of MOF crystals selectively and independently with different organic molecules.

Recently, Sharpless' "click" chemistry[10] has been suggested as an attractive vehicle for engendering chemical diversity in MOFs. Devic et al.[11] employed the click reaction pre-MOF synthesis to produce a novel flexible ligand, while we[9] and others[12] have performed this cycloaddition on previously assembled frameworks. Goto et al.[12] synthesized an azide-containing MOF material that may be modified directly, whereas we[9] constructed a permanently microporous, protected acetylene-bearing framework which requires deprotection of the acetylene ligands prior to undergoing the Cu^I-catalyzed cycloaddition (Figure 1A). This deprotection may be viewed as an activation step for the subsequent click reaction, and can be performed selectively to provide additional control over the manipulation of MOF properties. Previously, we were able to "activate" the exterior of MOF crystals exclusively by taking advantage of the prohibitively large size of the deprotecting agent.[9] While this tactic was successful, it can only work with MOFs that have relatively small pores and hence would be inapplicable to frameworks with larger cavities intended for additional interior functionalization. Accordingly, we sought a more general approach to limiting access of the deprotecting agent to the exterior surfaces of MOF crystals. One such strategy would involve undertaking the deprotection in a medium that is immiscible with the pore solvent, thus limiting the desilylation to the external surfaces of the MOF crystals. After the subsequent click reaction, the interior surfaces could be deprotected completely and "decorated" with a different azide (Figure 1B).

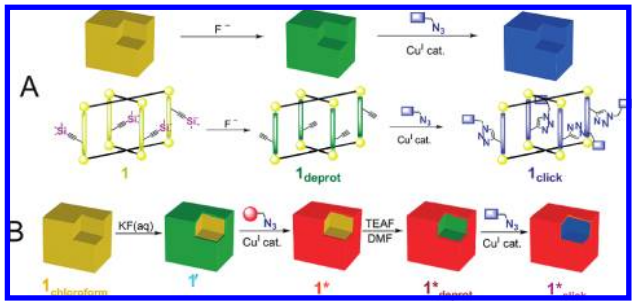

Figure 1. (A) Schematic illustration of the deprotection and subsequent "clicking" of a MOF crystal (top), and of a single unit cell of this MOF (**1**) undergoing the same reaction sequence (bottom). (B) Schematic representation of a strategy for functionalizing the internal and external surfaces of a crystal of **1** independently with two different azides.

In designing an acetylene-bearing MOF material whose crystals can be differentially functionalized on their internal and external surfaces, we required that the framework cavities be large enough to accommodate the click transition state made up by the alkyne, the azide, and the catalyst. Additionally, we aimed to construct a material that maintained its structural integrity after evacuation, as there is no example of a demonstrably *permanently* microporous MOF whose internal surfaces can be functionalized using click chemistry. Recently, we have had excellent success in assembling non-catenated, pillared, paddle-wheel MOF materials[13] by using 1,2,4,5-tetrakis(4-carboxyphenyl)benzene (**TCPB**)[14] as the carboxylate strut (Figure 1). Thus, we combined the trimethylsilane-protected ligand **L1** with the octa-oxygenated **TCPB** and Zn^{2+} in acidic DMF at 80 °C to obtain large block-like crystals after 1 day. Single-crystal X-ray diffraction analysis revealed a non-catenated, pillared paddlewheel framework that we term **TO-MOF** (**1**)[15] (Figure 2).

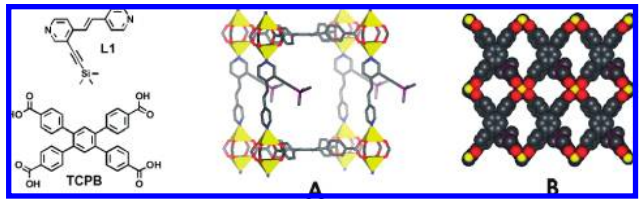

Figure 2. (A) Single network unit of **TO-MOF** (**1**), formed between **L1** and **TCPB**. (B) Crystal packing diagram of **TO-MOF** showing framework pores down the *c*-axis.

We were pleased to find that **1** can be easily made in bulk quantities (see Supporting Information (SI) and Figure 3A for

powder X-ray diffraction (PXRD) data). Thermogravimetric analysis (TGA, Figure 3B) and gas adsorption study (Figure 3C) of **1** indicate that it encloses large solvent-accessible volumes and is permanently microporous. However, before the large cavities of **1** could undergo the click reaction, the material had to be desilylated (to generate $\mathbf{1}_{\mathbf{deprot}}$). To this end, we used tetraethylammonium fluoride (TEAF) as our fluoride source for the removal of the trimethylsilyl (TMS) groups. Monitoring the infrared (IR) spectra of **1** during this reaction, we found that the C≡C stretch for **1** at 2155 cm^{-1} eventually shifted to 2105 cm^{-1}, indicating the complete conversion of a disubstituted alkyne to one that is monosubstituted, such as that in $\mathbf{1}_{\mathbf{deprot}}$ (Figure 3D). Additionally, the matrix-assisted laser desorption ionization time-of-flight (MALDI-TOF) mass spectrum of a pyridine solution of a partially dissolved crystal of **1** (Figure 3E) exhibited a significant peak for $\mathbf{L1}_{\mathbf{deprot}}$ (deprotected **L1** ($[M + H]^+ = 207$)); the peak for **L1** ($[M + H]^+ = 279$) was not apparent. Loss of the TMS group was corroborated by ^{1}H NMR data (Figure 3F), which showed the disappearance of the methyl protons. Powder X-ray diffraction (PXRD) data for isolated $\mathbf{1}_{\mathbf{deprot}}$ verified that the material was still crystalline after deprotection (Figure 2A), with many of the original peaks of **1** still present. Retention of porosity in $\mathbf{1}_{\mathbf{deprot}}$ was confirmed by performing thermogravimetric analysis (TGA, Figure 3B), as well as gas adsorption measurements (see Figure 3D (CO_2) and Figure S3 in SI (N_2)).

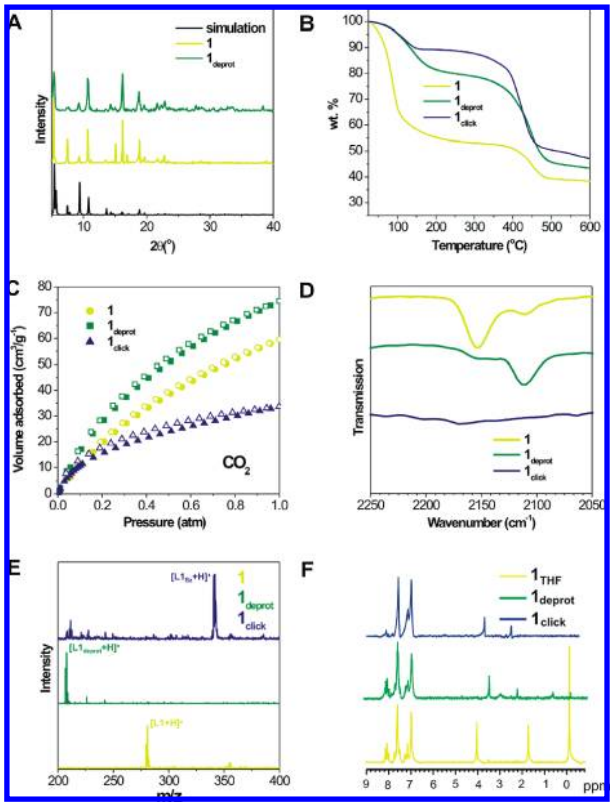

Figure 3. (A) PXRD data for **1** and $\mathbf{1}_{\mathbf{deprot}}$. (B−F) Characterization data for **1**, $\mathbf{1}_{\mathbf{deprot}}$, and $\mathbf{1}_{\mathbf{click}}$: (B) TGA, (C) CO_2 uptake (adsorption (closed) and desorption (open), (D) IR, (E) MALDI-TOF, and (F) ^{1}H NMR (D_2SO_4).

After successful deprotection of **TO-MOF** (**1**), we continued on to click $\mathbf{1}_{\mathbf{deprot}}$ with benzyl azide, which had been previously generated *in situ* using benzyl bromide and sodium azide. The click reaction was monitored by IR spectroscopy, and the data showed the expected disappearance of the monosubstituted C≡C stretch at 2105 cm^{-1} (Figure 3D). Analysis of a partially dissolved sample of the product $\mathbf{1}_{\mathbf{click}}$ by MALDI-TOF MS confirmed the formation of the benzyl-clicked ligand, $\mathbf{L1}_{\mathbf{Bz}}$ (Figure 3E). This triazole product of the cycloaddition of $\mathbf{L1}_{\mathbf{deprot}}$ and benzyl azide appeared as the major species in the mass spectrum ($[M + H]^+ = 340$), confirming the covalent attachment of benzyl azide to the deprotected MOF crystals. TGA (Figure 3B) and CO_2 adsorption data (Figure 3C) of $\mathbf{1}_{\mathbf{click}}$ indicated that the material was still porous with, as expected, reduced pore volume.[16]

In Figure 1B, we outline a strategy for clicking on the external surface of a MOF material an organic molecule that is different from another clicked to the MOF interior. We opted to take advantage of the poor solubility of KF in organic solvents to carry out the proposed selective deprotection: when the MOF channels are filled with chloroform, an aqueous solution of KF will not enter the pores, and KF will not partition into the organic solvent. As-synthesized **TO-MOF** (**1**) was first solvent-exchanged with chloroform and then agitated in an aqueous solution of KF, to afford the surface-deprotected **1′**. MALDI-TOF MS analysis was performed on pyridine solutions of partially dissolved samples of **1′**, with the spectrum showing peaks corresponding to the deprotected ligand $\mathbf{L1}_{\mathbf{deprot}}$ and its various adducts (Figure 4A: $[M + H]^+ = 207$; $[M + 2H + F]^+ = 227$; $[M + H + K + F]^+ = 265$). The corresponding ^{1}H NMR spectrum of D_2SO_4-dissolved **1′** (Figure 4B) indicated a negligible amount of ligand deprotection, a result that was corroborated by solid-state IR spectroscopy (Figure 4C).

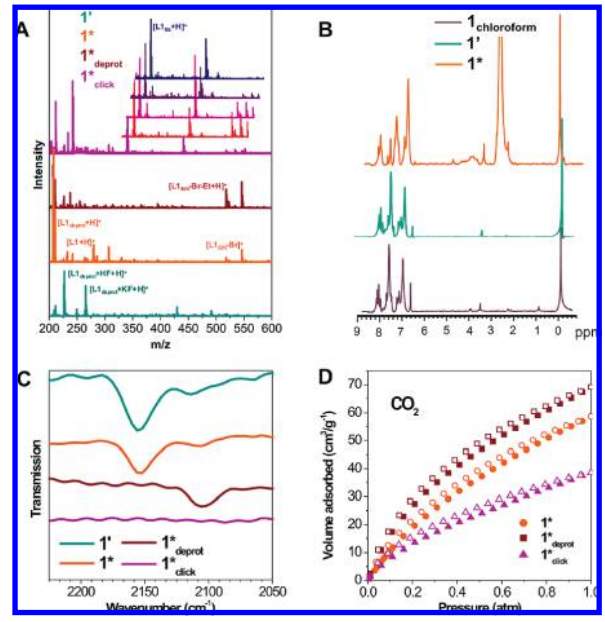

Figure 4. (A) MALDI-TOF mass spectra for **1′**, **1***, $\mathbf{1*}_{\mathbf{deprot}}$, and $\mathbf{1*}_{\mathbf{click}}$. (B) Solution ^{1}H NMR spectra for partially dissolved **1**, **1′** and **1***. (C) Solid-state IR spectra for **1′**, **1***, $\mathbf{1*}_{\mathbf{deprot}}$, and $\mathbf{1*}_{\mathbf{click}}$. (D) N_2 isotherms for **1** and **1*** (adsorption (closed) and desorption (open)).

With the aforementioned evidence for selective deprotection of the external surfaces of crystals of **1′** in hand, we moved on to click the dye ethidium bromide monoazide, $\mathbf{E}_{\mathbf{azide}}$, to these deprotected surfaces. We chose $\mathbf{E}_{\mathbf{azide}}$ primarily for visualization, but also because we have previously demonstrated its effectiveness in the functionalization of MOF surfaces.[9] The surface-clicked MOF, **1***, was characterized analytically to ensure covalent attachment of the dye, and to verify that the majority of the material was still protected. The MALDI-TOF mass spectrum of a pyridine solution of a partially dissolved sample of **1*** (Figure 4A) confirmed the presence of the triazole product of the click reaction, $\mathbf{L1}_{\mathbf{Eth}}$ ($[M - Br]^+ = 546$ and $[M - Br - CH_2CH_3 + H]^+ = 518$). At the same

time, solid-state IR (Figure 4C) and D_2SO_4-dissolved solution ^1H NMR (Figure 4B) spectra of **1*** indicated that most of the interior dipyridyl struts remain protected during the surface-click reaction, as expected.

With the composition of **1*** established, we were pleased to find that both PXRD and N_2 adsorption analyses of **1*** indicated that it is not significantly different from **1** in terms of internal structure: The positions of PXRD peaks are in agreement (Figure S2 in SI), and BET surface areas from N_2 adsorption isotherms match within 10% (680 m^2/g for **1** and 620 m^2/g for **1***, Figure S4 in SI).

In our hands, long-term deprotection of silylated MOFs using various fluoride sources can cause slight dissolution of the crystals. Given the possibility of the near-surface dye leaching due to this dissolution, we carried out the internal deprotection of **1*** using a more dilute solution of TEAF in THF (0.001 M for **1*** vs 0.01 M for **1**). If successful, this would afford $\mathbf{1^*_{deprot}}$, a surface-clicked and interior-deprotected version of **TO-MOF**. Monitoring the deprotection by solid-state IR spectroscopy indicated the complete conversion of disubstituted triple bonds to terminal alkynes (Figure 4C). Additionally, the MALDI-TOF mass spectrum of a sample of $\mathbf{1^*_{deprot}}$ partially dissolved in pyridine (Figure 4A) still had peaks corresponding to the surface-clicked $\mathbf{L1_{Eth}}$ triazole product ($[M - Br]^+ = 546$ and $[M - Br - CH_2CH_3 + H]^+ = 518$).

To functionalize the interior of $\mathbf{1^*_{deprot}}$, we again utilized benzyl azide, hoping to achieve the differentially functionalized MOF, $\mathbf{1^*_{click}}$. After treating $\mathbf{1^*_{deprot}}$ with benzyl azide under click conditions for 72 h, the MALDI-TOF mass spectrum of the partially dissolved product showed triazole products from $\mathbf{L1_{deprot}}$ reacting with both benzyl azide and $\mathbf{E_{azide}}$, and only a negligible amount of $\mathbf{L1_{deprot}}$ (Figure 4A). The MALDI-TOF spectra of successive pyridine dissolutions of this $\mathbf{1^*_{click}}$ material confirm its "core-shell" composition: peaks corresponding to $\mathbf{L1_{Eth}}$ (shell-clicked region) gradually diminish in intensity compared to the peak for $\mathbf{L1_{Bz}}$ (core-clicked region) and eventually become unobservable. The solid-state IR spectrum of the crude MOF product indicates that no unreacted alkyne remains (Figure 4C).

By exploiting both the solid-state properties and the synthetic tunability of metal-organic framework materials, we have produced a highly tailored, microporous, crystalline MOF material. While the organic moieties used to functionalize **TO-MOF** in "core-shell" fashion were chosen only to demonstrate the feasibility, the results open up a host of possibilities accessible through this methodology. For example, one could imagine synthesizing a variety of drugs that are linked to an azide via an acid-labile linker, and then clicking them to the inside of MOF crystallites whose surfaces have been decorated with targeting groups.[17] However this strategy may be employed in the future, the work reported herein clearly demonstrates the advantage of bringing synthetic organic tools and strategies to bear when developing new MOF materials.

Acknowledgment. We acknowledge financial support from the Northwestern Institute for Catalysis in Energy Processes, DTRA/ARO, AFOSR, and the Northwestern Nanoscale Science and Engineering Center. Crystallographic work at the Advanced Photon Source (APS) at Argonne National Laboratory was conducted at ChemMatCARS Sector 15, principally supported by NSF/Department of Energy (DOE) under Grant Number CHE-0535644. The APS is supported by the DOE, Office of Basic Energy Sciences (Contract No. DE-AC02-06CH11357). NMR and MALDI data were collected at Northwestern's IMSERC facility.

Supporting Information Available: Preparation and N_2 adsorption data of **1**, $\mathbf{1_{deprot}}$, $\mathbf{1_{click}}$, **1′**, **1***, $\mathbf{1^*_{deprot}}$, and $\mathbf{1^*_{click}}$. TGA data for evacuated and resolvated **1**, $\mathbf{1_{deprot}}$, and $\mathbf{1_{click}}$, and PXRD data for resolvated **1** and $\mathbf{1_{deprot}}$; structural characterization details (single-crystal X-ray diffraction, PXRD, MALDI, ^1H NMR, IR, TGA, and gas adsorption). This material is available free of charge via the Internet at http://pubs.acs.org.

References

(1) (a) Rowsell, J. L. C.; Millward, A. R.; Park, K. S.; Yaghi, O. M. *J. Am. Chem. Soc.* **2004**, *126*, 5666–5667. (b) Eddaoudi, M.; Kim, J.; Rosi, N.; Vodak, D.; Wachter, J.; O'Keeffe, M.; Yaghi Omar, M. *Science* **2002**, *295*, 469–472. (c) Ma, B.-Q.; Mulfort, K. L.; Hupp, J. T. *Inorg. Chem.* **2005**, *44*, 4912–4914.

(2) (a) Lin, X.; Jia, J.; Zhao, X.; Thomas, K. M.; Blake, A. J.; Walker, G. S.; Champness, N. R.; Hubberstey, P.; Schroeder, M. *Angew. Chem., Int. Ed.* **2006**, *45*, 7358–7364. (b) Furukawa, H.; Kim, J.; Ockwig, N. W.; O'Keeffe, M.; Yaghi, O. M. *J. Am. Chem. Soc.* **2008**, *130*, 11650–11661.

(3) (a) Seo, J. S.; Whang, D.; Lee, H.; Jun, S. I.; Oh, J.; Jeon, Y. J.; Kim, K. *Nature* **2000**, *404*, 982–986. (b) Wu, C.-D.; Hu, A.; Zhang, L.; Lin, W. *J. Am. Chem. Soc.* **2005**, *127*, 8940–8941. (c) Cho, S.-H.; Ma, B.; Nguyen, S. T.; Hupp, J. T.; Albrecht-Schmitt, T. E. *Chem. Commun.* **2006**, 2563–2565.

(4) (a) Burrows, A. D.; Frost, C.; Mahon, M. F.; Richardson, C. *Angew. Chem., Int. Ed.* **2008**, *47*, 8482–8486. (b) Gadzikwa, T.; Farha, O. K.; Mulfort, K. L.; Hupp, J. T.; Nguyen, S. T. *Chem. Commun.* **2009**, 3720–3722.

(5) (a) Dugan, E.; Wang, Z.; Okamura, M.; Medina, A.; Cohen, S. M. *Chem. Commun.* **2008**, 3366–3368. (b) Tanabe, K. K.; Wang, Z.; Cohen, S. M. *J. Am. Chem. Soc.* **2008**, *130*, 8508–8517. (c) Wang, Z.; Cohen, S. M. *J. Am. Chem. Soc.* **2007**, *129*, 12368–12369. (d) Wang, Z.; Cohen, S. M. *Angew. Chem., Int. Ed.* **2008**, *47*, 4699–4702. (e) Wang, Z.; Cohen, S. M. *Chem. Soc. Rev.* **2009**, *38*, 1315–1329. (f) Wang, Z.; Tanabe, K. K.; Cohen, S. M. *Inorg. Chem.* **2009**, *48*, 296–306.

(6) (a) Costa, J. S.; Gamez, P.; Black, C. A.; Roubeau, O.; Teat, S. J.; Reedijk, J. *Eur. J. Inorg. Chem.* **2008**, 1551–1554. (b) Haneda, T.; Kawano, M.; Kawamichi, T.; Fujita, M. *J. Am. Chem. Soc.* **2008**, *130*, 1578–1579. (c) Hwang, Y. K.; Hong, D.-Y.; Chang, J.-S.; Jhung, S. H.; Seo, Y.-K.; Kim, J.; Vimont, A.; Daturi, M.; Serre, C.; Ferey, G. *Angew. Chem., Int. Ed.* **2008**, *47*, 4144–4148. (d) Kawamichi, T.; Kodama, T.; Kawano, M.; Fujita, M. *Angew. Chem., Int. Ed.* **2008**, *47*, 8030–8032. (e) Kaye, S. S.; Long, J. R. *J. Am. Chem. Soc.* **2008**, *130*, 806–807. (f) Morris, W.; Doonan, C. J.; Furukawa, H.; Banerjee, R.; Yaghi, O. M. *J. Am. Chem. Soc.* **2008**, *130*, 12626–12627.

(7) (a) Mulfort, K. L.; Hupp, J. T. *J. Am. Chem. Soc.* **2007**, *129*, 9604–9605. (b) Mulfort, K. L.; Hupp, J. T. *Inorg. Chem.* **2008**, *47*, 7936–7938. (c) Mulfort, K. L.; Wilson, T. M.; Wasielewski, M. R.; Hupp, J. T. *Langmuir* **2009**, *25*, 503–508.

(8) Ingleson, M. J.; Barrio, J. P.; Guilbaud, J.-B.; Khimyak, Y. Z.; Rosseinsky, M. J. *Chem. Commun.* **2008**, 2680–2682.

(9) Gadzikwa, T.; Lu, G.; Stern, C. L.; Wilson, S. R.; Hupp, J. T.; Nguyen, S. T. *Chem. Commun.* **2008**, 5493–5495.

(10) (a) Kolb, H. C.; Finn, M. G.; Sharpless, K. B. *Angew. Chem., Int. Ed.* **2001**, *40*, 2004–2021. (b) Wu, P.; Fokin, V. V. *Aldrichchimica Acta* **2007**, *40*, 7–17.

(11) Devic, T.; David, O.; Valls, M.; Marrot, J.; Couty, F.; Ferey, G. *J. Am. Chem. Soc.* **2007**, *129*, 12614–12615.

(12) Goto, Y.; Sato, H.; Shinkai, S.; Sada, K. *J. Am. Chem. Soc.* **2008**, *130*, 14354–14355.

(13) (a) Mulfort, K. L.; Farha, O. K.; Stern, C. L.; Sarjeant, A. A.; Hupp, J. T. *J. Am. Chem. Soc.* **2009**, *131*, 3866–3868. (b) Shultz, A. M.; Farha, O. K.; Hupp, J. T.; Nguyen, S. T. *J. Am. Chem. Soc.* **2009**, *131*, 4204–4205.

(14) Farha, O. K.; Mulfort, K. L.; Hupp, J. T. *Inorg. Chem.* **2008**, *47*, 10223–10225.

(15) Triclinic space group $P\bar{1}$ with $Z = 1$, $a = 11.8137(8)$ Å, $b = 15.5303(11)$ Å, $c = 16.3912(15)$ Å, $\alpha = 90.00°$ $\beta = 90.00°$, $\gamma = 90.00°$, $V = 3007.3(4)$ Å^3, 34398 reflections collected with 17529 unique reflections [$R_{int} = 0.0597$], 98.6% completeness to $\theta = 25.00°$, Goodness-of-fit on F_2 was 0.935, $R_{obs} = 0.0696$, $wR_{obs} = 0.1660$ for reflections above $2\sigma(I)$, $R_{all} = 0.0894$, $wR_{all} = 0.1767$ for all data, and min/max residual electron density of 0.912 and -0.642 e•Å^{-3}, respectively.

(16) ^1H NMR analysis of the dissociated MOF was of limited utility due to the insolubility of $L1_{Bz}$ in all solvents employed. Diminished pyridyl peaks point indirectly to the conversion of the majority of $L1_{deprot}$ to the cycloaddition adduct (Figure 3F).

(17) For examples of MOFs as potential drug delivery vehicles, see: (a) Horcajada, P.; Serre, C.; Vallet-Regi, M.; Sebban, M.; Taulelle, F.; Ferey, G. *Angew. Chem., Int. Ed.* **2006**, *45*, 5974–5978. (b) Rieter, W. J.; Taylor, K. M. L.; Lin, W. *J. Am. Chem. Soc.* **2007**, *129*, 9852–9853. (c) Horcajada, P.; Serre, C.; Maurin, G.; Ramsahye, N. A.; Balas, F.; Vallet-Regi, M.; Sebban, M.; Taulelle, F.; Ferey, G. *J. Am. Chem. Soc.* **2008**, *130*, 6774–6780.

JA904189D